October, 2007

Platinum Nanoparticle Shape Effects on Benzene Hydrogenation Selectivity

Kaitlin M. Bratlie, *University of California - Berkeley*
Hyunjoo Lee, *University of California - Berkeley*
Kyriakos Komvopoulos, *University of California - Berkeley*
Peidong Yang, *University of California - Berkeley*
Gabor A. Somorjai, *University of California - Berkeley*

NANO LETTERS

2007
Vol. 7, No. 10
3097−3101

Platinum Nanoparticle Shape Effects on Benzene Hydrogenation Selectivity

Kaitlin M. Bratlie,[†,‡] Hyunjoo Lee,[†] Kyriakos Komvopoulos,[‡] Peidong Yang,[†] and Gabor A. Somorjai*[,†]

Department of Chemistry, University of California, Berkeley, California 94720, and Materials Sciences Division, Lawrence Berkeley National Laboratory, Berkeley, California 94720, Department of Mechanical Engineering, University of California, Berkeley, California 94720

Received July 3, 2007; Revised Manuscript Received August 27, 2007

ABSTRACT

Benzene hydrogenation was investigated in the presence of a surface monolayer consisting of Pt nanoparticles of different shapes (cubic and cuboctahedral) and tetradecyltrimethylammonium bromide (TTAB). Infrared spectroscopy indicated that TTAB binds to the Pt surface through a weak C–H···Pt bond of the alkyl chain. The catalytic selectivity was found to be strongly affected by the nanoparticle shape. Both cyclohexane and cyclohexene product molecules were formed on cuboctahedral nanoparticles, whereas only cyclohexane was produced on cubic nanoparticles. These results are the same as the product selectivities obtained on Pt(111) and Pt(100) single crystals in earlier studies. The apparent activation energy for cyclohexane production on cubic nanoparticles is 10.9 ± 0.4 kcal/mol, while for cuboctahedral nanoparticles, the apparent activation energies for cyclohexane and cyclohexene production are 8.3 ± 0.2 and 12.2 ± 0.4 kcal/mol, respectively. These activation energies are lower, and corresponding turnover rates are three times higher than those obtained with single-crystal Pt surfaces.

Structure-insensitive reactions on Pt nanoparticles, such as ethylene hydrogenation, have been the main objective of numerous investigations.[1−4] Extending reaction studies to structure-sensitive reactions for which turnover rates and product selectivities change with both nanoparticle size and shape is essential for obtaining a molecular understanding of catalytic processes. Benzene hydrogenation is an ideal reaction for such studies as it has been investigated extensively on single-crystalline Pt surfaces.[5−7] Because this reaction has been shown to produce only cyclohexane on Pt(100) and both cyclohexene and cyclohexane on Pt(111),[6] it is suitable for probing nanoparticle shape-dependent reaction selectivity in catalysis. The objective of this investigation was to examine the catalytic activity of benzene hydrogenation on surface monolayers consisting of cubic or cuboctahedral Pt nanoparticles and tetradecyltrimethylammonium bromide (TTAB) capping agent. Kinetic results for TTAB-stabilized Pt nanoparticles are contrasted with those of single-crystal Pt surfaces to elucidate nanoparticle shape effects on catalysis.

The stabilizing agent used to prevent nanoparticle aggregation can have consequential effects on the catalytic activity. Strongly bound stabilizing agents may hinder or even prevent catalysis by blocking active surface sites and inducing steric effects. For example, previous work[8] has shown that certain stabilizers that strongly encapsulate Pd nanoparticles prevent catalysis. TTAB has recently been used as a stabilizing agent in Pt nanoparticle synthesis and was found to produce much higher catalytic activity for ethylene hydrogenation than poly(vinylpyrrolidone) stabilizing agent.[9] However, the interaction of TTAB with the Pt surface has not been studied yet. Infrared (IR) spectra provide insight into this interaction in a dry condition that is conducive to gas-phase reaction.

The Pt nanoparticles used in the present reaction studies are shown in Figure 1. The synthesis of these particles has been reported in a previous study.[9] The cubic particles have a size of 12.3 ± 1.4 nm (diagonal, 79% cubes, 3% triangles, and 18% irregular shapes) and consist of only Pt(100), whereas the cuboctahedral particles have a size of 13.5 ± 1.5 nm (vertex to vertex, 90% cuboctahedra and 10% irregular shapes) and consist of both Pt(100) and Pt(111). Unlike cubic nanoparticles, the (111) surface in cuboctahedral nanoparticles would promote the production of cyclohexene. Monolayers of these nanoparticles were prepared on Si wafers for reaction studies by the Langmuir−Blodgett technique, as illustrated in detail in the Supporting Information of this article. Figure 2 shows a comparison between kinetic data of TTAB-stabilized cubic and cuboctahedral Pt nanoparticles in the temperature range of 310−400 K for

* To whom correspondence should be addressed. E-mail: somorjai@socrates.berkeley.edu (G.A.S.); kmbratlie@lbl.gov (K.M.B.). Telephone: 510-642-4053 (G.A.S.). Fax: 510-643-9668 (G.A.S.).
† Department of Chemistry.
‡ Department of Mechanical Engineering.

10.1021/nl0716000 CCC: $37.00
Published on Web 09/18/2007

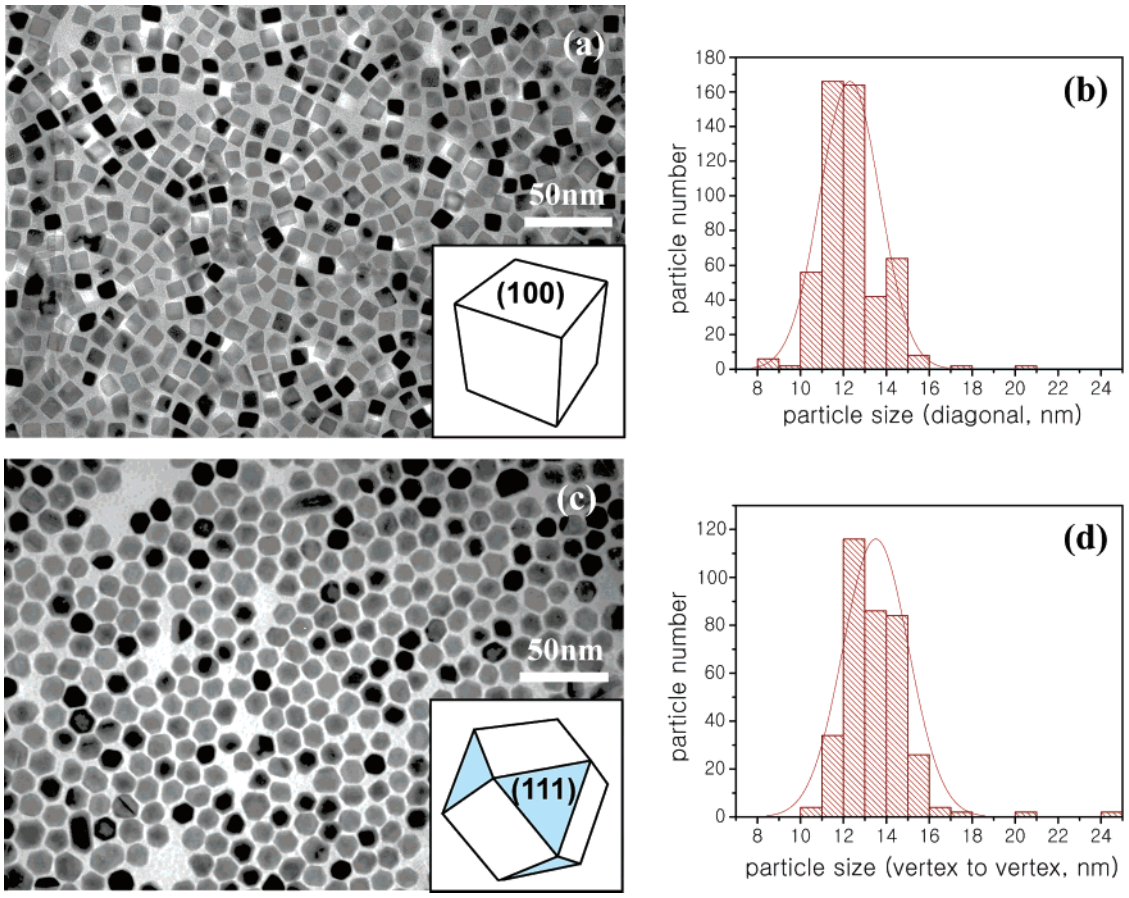

Figure 1. (a) TEM image and (b) size distribution of TTAB-stabilized cubic particles (average size: 12.3 ± 1.4 nm, 79% cubes, 3% triangles, and 18% irregular shapes). (c) TEM image and (d) size distribution of TTAB-stabilized cuboctahedral particles (average size: 13.5 ± 1.5 nm, 90% cuboctahedra and 10% irregular shapes).

10 Torr C_6H_6, 100 Torr H_2, and 650 Torr Ar. It is noted that only cyclohexane formed on cubic nanoparticles, as opposed to both cyclohexane and cyclohexene on cuboctahedral nanoparticles. The calculation of the turnover rates shown in Figure 2a was based on the nanoparticle coverage of the Si wafer surface determined from SEM images, assuming that each Pt atom at the monolayer surface is an active site. The error bars indicate the image-to-image scatter in the measurements. Figure 2b shows Arrhenius plots of cyclohexane and cyclohexene turnover rates in the 310−400 K temperature range. The deviation of both cyclohexane and cyclohexene turnover rates from the Arrhenius relationship above ~340 and ~360 K, respectively, is attributed to changes in the Pt surface coverage caused by gas-phase adsorbed species, as discussed previously.[10] The apparent activation energies for cyclohexane and cyclohexene formation on cuboctahedral nanoparticles in the temperature ranges of 310−340 and 330−360 K are respectively equal to 8.3 ± 0.2 and 12.2 ± 0.4 kcal/mol. For cubic nanoparticles, the apparent activation energy for cyclohexane formation in the temperature range of 330−370 K is equal to 10.9 ± 0.4 kcal/mol. The SEM images (Figure S1 in the Supporting Information) obtained before and after reaction at 400 K reveal that nanoparticle aggregation did not occur under the present reaction conditions. In addition, transmission electron microscopy (TEM) did not reveal any discernible changes in nanoparticle shape after reaction. Figure 3 shows representative TEM images of cubic and cuboctahedral Pt nanoparticles obtained after reaction at 400 K, which confirm that the observed chemistry was a result of differences in the original nanoparticle shape, not a consequence of nanoparticle shape changes induced during the reaction.

Previous studies[5,6] of benzene hydrogenation on single-crystal Pt surfaces have demonstrated that, unlike cyclohexene, low-temperature production of cyclohexane is not structure-sensitive, as evidenced by the formation of both cyclohexene and cyclohexane on Pt(111) and only cyclohexane on Pt(100). The formation of these products on TTAB-stabilized nanoparticles is in agreement with the former findings.

Table 1 shows the effect of the nanoparticle shape on the apparent activation energy and maximum turnover rate of cyclohexane and cyclohexene. For comparison, similar data for single-crystal Pt(100) and Pt(111) surfaces reported previously[5,6] are also included in Table 1. The apparent activation energy for cyclohexane formation on the cubic nanoparticles comprising only {100} facets is less than that of Pt(100). Similarly, the apparent activation energies for cyclohexane and cyclohexene formation on the cuboctahedral nanoparticles are less than that of Pt(111). A 3-fold increase in the turnover rate was also observed for benzene hydrogenation on nanoparticles compared to single-crystal Pt

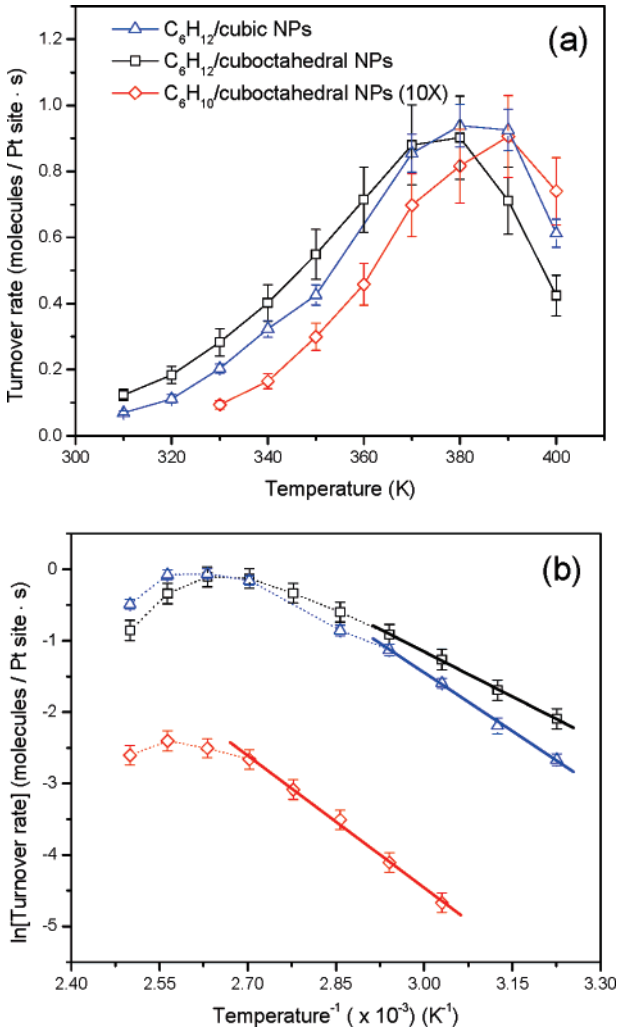

Figure 2. (a) Turnover rates of cyclohexane (C_6H_{12}) and cyclohexene (C_6H_{10}) formation on TTAB-stabilized cubic and cuboctahedral Pt nanoparticles (NPs) for 10 Torr C_6H_6, 100 Torr H_2, and 650 Torr Ar, and (b) corresponding Arrhenius plots. The deviation from the Arrhenius behavior above 340 K for cyclohexane and above 370 K for cyclohexene formation is attributed to changes in the nanoparticle surface coverage caused by gas-phase adsorbates. The dotted lines are drawn as visual aides.

surfaces. This can be seen by comparing the kinetic data and Arrhenius plots for benzene hydrogenation on single-crystal Pt(100) and Pt(111) surfaces shown in Figure 4. The lower apparent activation energies and higher turnover rates obtained with nanoparticles than single crystals may be attributed to an increase in corner and edge sites. The ratio of corner and edge atoms to terrace atoms increases with the decrease of crystal domains.[11−14] Edge and corner atoms exhibit open coordination sites that may result in significantly different bond enthalpies, desorption energies, and adsorption geometries compared to adsorption on terrace sites. Another possible explanation is the change in the electronic structure with decreasing size. Electronic changes due to Pd nanoparticle size changes have been reported for formic acid oxidation.[15] The smallest particles were found to be the most active, which was attributed to an enhancement of the d-band hybridization that weakened the bond strength of the COOH intermediate with the surface of the Pd nanoparticles.

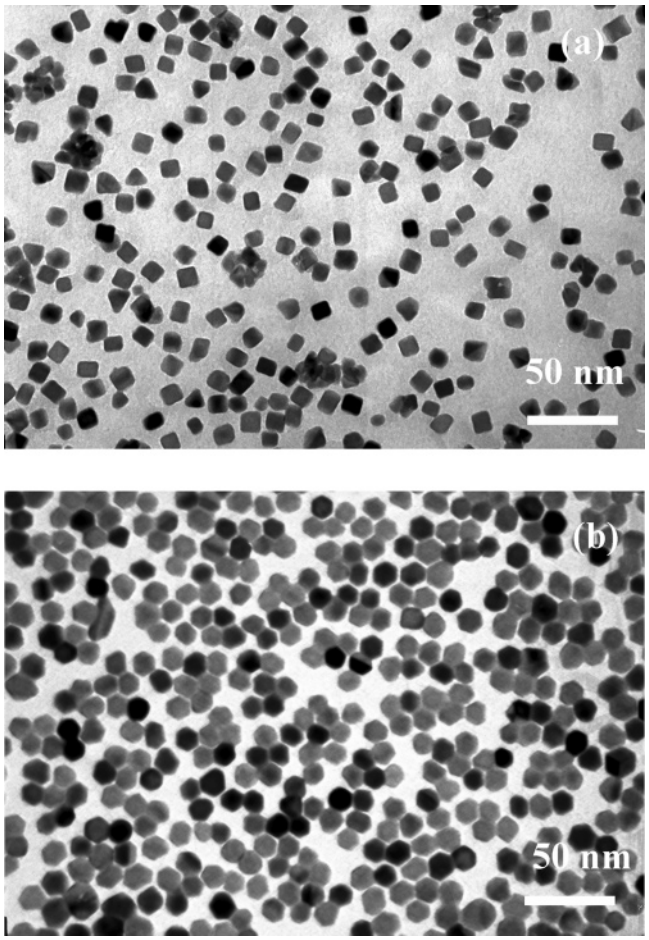

Figure 3. TEM images of TTAB-stabilized (a) cubic and (b) cuboctahedral Pt nanoparticles after reaction at 400 K for 10 Torr C_6H_6, 100 Torr H_2, and 650 Torr Ar.

Compared to single crystals, a 3-fold increase in the turnover rate for benzene hydrogenation was also observed in the presence of nanoparticles. This increase is also attributed to an increase of the ratio of corner and edge atoms to terrace atoms or a change in electronic structure with decreasing crystal size. Benzene hydrogenation may be augmented at edge and corner sites, thus increasing the catalytic activity of the nanoparticles.

IR spectra of pure TTAB and TTAB-stabilized cubic Pt nanoparticles revealed insignificant differences in the C−H rocking (700−740 cm^{-1}), C−H bending (1350−1550 cm^{-1}), and C−N$^+$ stretching (880−1000 cm^{-1}) regions. These spectral windows along with their peak assignments can be found in the Supporting Information (Figure S2 and Table S1). However, the IR spectra in the C−H stretching region shown in Figure 5 show significant differences in the spectra of pure TTAB and TTAB-stabilized nanoparticles. The IR spectrum of the TTAB-stabilized nanoparticles contains an additional mode at 2783 cm^{-1}, which is attributed to direct C−H···M (M = metal) interactions between Pt atoms on the nanoparticle surfaces and proximal C−H bonds [ν(C−$H_{proximal}$)][16] and is usually referred to as "softened" mode. This mode generally indicates a direct interaction of the alkyl chain with the metal surface.[16] The assignment of each peak in the spectra of Figure 5 can also be found in the Supporting

Table 1. Apparent Activation Energy and Maximum Turnover Rate for TTAB-Stabilized Pt Nanoparticles (NPs) and Pt Single-Crystals

property	reaction product	TTAB-stabilized Pt NPs		Pt single crystals[5,6]	
		cubic	cuboctahedral	Pt(100)	Pt(111)
apparent activation energy[a] (kcal/mol)	cyclohexane	10.9 ± 0.4	8.3 ± 0.2	15.7 ± 0.1	9.8 ± 0.1
	cyclohexene	na	12.2 ± 0.4	na	18.3 ± 0.8
maximum turnover rate[b] (molecules/Pt site·s)	cyclohexane	0.93 ± 0.06	0.90 ± 0.12	0.27 ± 0.01	0.30 ± 0.01
	cyclohexene	na	0.08 ± 0.01	na	0.015 ± 0.002

[a] Measured in the temperature range of 310−400 K. [b] Measured at 380 K for Pt NPs and 420 K for Pt single crystals.

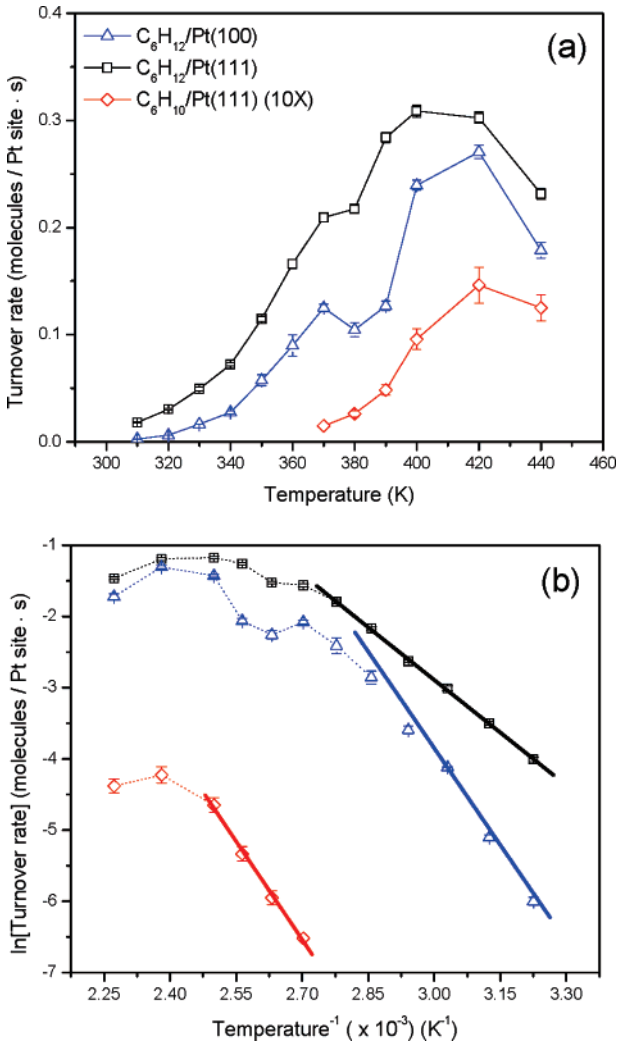

Figure 4. (a) Turnover rates of cyclohexane (C_6H_{12}) and cyclohexene (C_6H_{10}) formation on Pt(100) and Pt(111) single-crystals for 10 Torr C_6H_6, 100 Torr H_2, and 650 Torr Ar and (b) corresponding Arrhenius plots. The dotted lines are drawn as visual aides.

Information (Table S1). Because the IR spectra of pure TTAB and TTAB-stabilized cubic Pt nanoparticles differ only in the C−H stretching region, it may be presumed that TTAB does not interact with the Pt surface through the trimethylammonium head group but rather through the alkyl chain, as indicated by the "softened" C−H mode in a dry condition. The different interaction of alkylammonium ions on Pt surfaces compared to Au surfaces[17] may be related to the catalytic activity of Pt toward alkanes, which allows Pt to more readily dehydrogenate alkanes than Au.

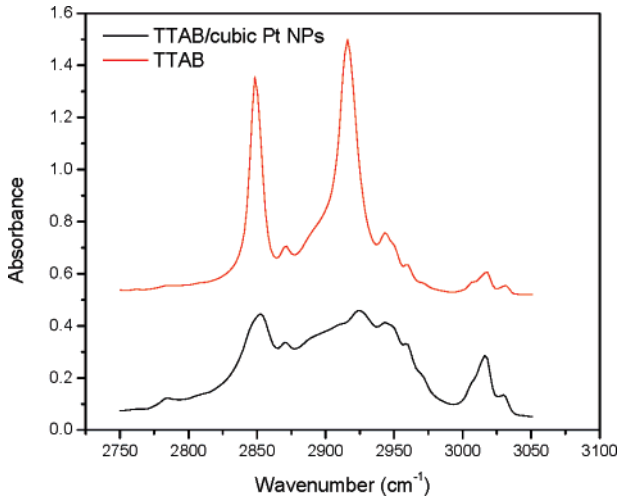

Figure 5. IR spectra of pure TTAB and TTAB-stabilized cubic nanoparticles (NPs) in the C−H stretching region. Mode assignments (based on information from the literature) are given in Supporting Information (Table S1).

In this investigation, nanoparticle surface effects on benzene hydrogenation were studied by comparing kinetic results for cubic and cuboctahedral Pt nanoparticles. It was found that the capping agent (TTAB) interacts with the Pt atoms through the alkyl chain forming C−H···Pt weak bonds. Benzene hydrogenation studies demonstrated that both cyclohexene and cyclohexane formed on cuboctahedral nanoparticles and only cyclohexane on cubic nanoparticles, consistent with previous results for single-crystal Pt surfaces. The significantly lower apparent activation energies and higher turnover rates obtained with Pt nanoparticles than Pt single crystals may be attributed to an increase of the corner and edge sites on the nanoparticles available for catalysis or changes in the electronic structure of the nanoparticles compared to the Pt single crystals.

Acknowledgment. This work was supported by the Berkeley-ITRI Research Center (BIRC) under fund no. 46101-23845-44-EKMAJ, and the Director, Office of Energy Research, Office of Basic Energy Sciences, and Materials Science Division of the U.S. Department of Energy under contract no. DE-AC02-05CH11231.

Supporting Information Available: Experimental details describing synthesis, reaction studies, and infrared spectroscopic studies. This material is available free of charge via the Internet at http://pubs.acs.org.

References

(1) Chotisuwan, S.; Wittayakun, J.; Gates, B. C. *J. Phys. Chem. B* **2006**, *110*, 12459−12469.
(2) Contreras, A. M.; Grunes, J.; Yan, X. M.; Liddle, A.; Somorjai, G. A. *Top. Catal.* **2006**, *39*, 123−129.
(3) Gomez, R.; Solla-Gullon, J.; Perez, J. M.; Aldaz, A. *ChemPhysChem* **2005**, *6*, 2017−2021.
(4) Rioux, R. M.; Song, H.; Grass, M.; Habas, S.; Niesz, K.; Hoefelmeyer, J. D.; Yang, P.; Somorjai, G. A. *Top. Catal.* **2006**, *39*, 167−174.
(5) Bratlie, K. M.; Flores, L. D.; Somorjai, G. A. *J. Phys. Chem. B* **2006**, *110*, 10051−10057.
(6) Bratlie, K. M.; Kliewer, C. J.; Somorjai, G. A. *J. Phys. Chem. B* **2006**, *110*, 17925−17930.
(7) Bratlie, K. M.; Montano, M. O.; Flores, L. D.; Paajanen, M.; Somorjai, G. A. *J. Am. Chem. Soc.* **2006**, *128*, 12810−12816.
(8) Li, Y.; El-Sayed, M. A. *J. Phys. Chem. B* **2001**, *105*, 8938−8943.
(9) Lee, H.; Habas, S. E.; Kweskin, S. J.; Butcher, D.; Somorjai, G. A.; Yang, P. *Angew. Chem., Int. Ed.* **2006**, *45*, 7824−7828.
(10) Bratlie, K. M.; Flores, L. D.; Somorjai, G. A. *Surf. Sci.* **2005**, *599*, 93−106.
(11) Burton, J. J. *Cat. Rev.—Sci. Eng.* **1974**, *9*, 209−222.
(12) Greegor, R. B.; Lytle, F. W. *J. Catal.* **1980**, *63*, 476−486.
(13) Ladas, S. *Surf. Sci.* **1986**, *175*, L681−L686.
(14) Van Hardeveld, R.; Hartog, F. *Surf. Sci.* **1969**, *15*, 189.
(15) Zhou, W. P.; Lewera, A.; Larsen, R.; Masel, R. I.; Bagus, P. S.; Wieckowski, A. *J. Phys. Chem. B* **2006**, *110*, 13393−13398.
(16) Manner, W. L.; Bishop, A. R.; Girolami, G. S.; Nuzzo, R. G. *J. Phys. Chem. B* **1998**, *102*, 8816−8824.
(17) Nikoobakht, B.; El-Sayed, M. A. *Langmuir* **2001**, *17*, 6368−6374.

NL0716000